www.czasopisma.pan.pl PAN POLSKA AKADEMIA NAUK www.journals.pan.pl

BULLETIN OF THE POLISH ACADEMY OF SCIENCES
TECHNICAL SCIENCES, Vol. 65, No. 4, 2017
DOI: 10.1515/bpasts-2017-0051

Non-adaptive velocity tracking controller for a class of vehicles

P. HERMAN* and W. ADAMSKI

Poznan University of Technology, 3A Piotrowo St., 60-965 Poznan, Poland

Abstract. A non-adaptive controller for a class of vehicles is proposed in this paper. The velocity tracking controller is expressed in terms of the transformed equations of motion in which the obtained inertia matrix is diagonal. The control algorithm takes into account the dynamics of the system, which is included into the velocity gain matrix, and it can be applied for fully actuated vehicles. The considered class of systems includes underwater vehicles, fully actuated hovercrafts, and indoor airship moving with low velocity (below 3 m/s) and under assumption that the external disturbances are weak. The stability of the system under the designed controller is demonstrated by means of a Lyapunov-based argument. Some advantages arising from the use of the controller as well as the robustness to parameters uncertainty are also considered. The performance of the proposed controller is validated via simulation on a 6 DOF robotic indoor airship as well as for underwater vehicle model.

Key words: marine vehicle, fully actuated hovercraft, indoor airship, non-adaptive control, quasi-velocities, diagonal inertia matrix.

1. Introduction

The use of robotic marine vehicles, ground vehicles and air vehicles for different applications has been growing in the last decades. One of their advantages is low cost as compared to full scale and fully manned vessels. The setpoint, trajectory tracking and path following control strategies for robotic vehicles have received increased attention of researchers.

Numerous control algorithms have been proposed for the class of vehicles considered here. Tracking strategies related to underwater vehicles are presented, e.g., in [1–4]. Some control strategies for surface vessel including ships and hovercrafts can be found in [5–15]. Tracking controllers useful for marine vessels are described also in [16–20]. Referring to the airship trajectory tracking problem control algorithms are shown, e.g., in [21–24].

There are vehicles which, due to their construction, can be regarded as fully actuated. One may refer to the following works concerning underwater vehicles [1, 3, 25–29], surface vehicles [10, 30, 31, 15], hovercrafts [32, 33], and airships [34–36].

Velocity tracking control algorithms are rather rarely presented in the robotic literature as far as marine or aerial vehicles are concerned. However, tracking control strategies suitable for underwater vehicles or surface ships are shown, e.g., in [18, 37]. The velocity controllers related to velocity tracking for this class of vehicles are given in [38, 39]. The same type of controller for underwater vehicles are presented in [40]. The sliding mode control based approaches for velocity tracking for unmanned surface vessels are considered, e.g., in [6, 41, 42]. Moreover, velocity control algorithms are useful for other mechanical systems as unmanned helicopters [43] or quad-rotors [44]. Velocities are applied also for mobile platform control [45]. The tracking control algorithms for aerial indoor blimp using velocity-based controller are introduced in [21, 22].

In this paper a velocity control algorithm realized in the body-fixed frame for a class of fully actuated vehicles is introduced and discussed. The considered method is recommended for control of underwater vehicles, hovercrafts, or indoor airship moving slowly (with linear velocity below 3 m/s) and under assumption that the external disturbances are weak (if they can be omitted in equations of motion). It means that the submarine moves in calm water or the airship flies inside the hall. This velocity tracking controller is based on a velocity variables transformation arising from the inertia matrix decomposition. Therefore, the vehicle equations of motion are transformed into a velocity space. As a result, the obtained differential equations allow us to track the moving object velocity. It is noticeable that after the system inertia matrix decomposition the obtained controller includes the dynamic parameters set of the vehicle. Additionally, each rate is regulated separately in a sense (dynamical couplings are shifted to the appropriate velocity variable). One of benefits relies on that the system response of the system is fast and the velocity error convergence is quick. Consequently, the desired trajectory is reached in short time. Another advantage arising from the use of the controller is that the gain matrix related to the velocity error includes the system parameters highly dependent on the vehicle dynamics (for various vehicles the control coefficients can be different).

The novelty of the presented strategy is that the nonlinear controller is realized after transformation of equations of motion arising from the inertia matrix decomposition. Moreover, the proposed controller is universal in the following sense. First, it is suitable both for 6 DOF and for vehicles moving in the horizontal or vertical plane. Second, it can be applied in the same general (or reduced to 3 DOF) form for fully actuated marine vehicles, hovercrafts, and indoor airships. Third, some

*e-mail: przemyslaw.herman@put.poznan.pl

Manuscript submitted 2016-09-01, revised 2016-12-22, initially accepted for publication 2016-12-27, published in August 2017.

controllers which have simpler form can be deduced from it (particular cases of the controller). The stability of the vehicle under the controller is shown based on the Lyapunov argument. Additionally, the robustness to the system parameter changes is considered.

The mathematical model describing the dynamics and kinematics of the class of vehicles is introduced in Section 2. The proposed velocity tracking controller is presented and considered in Section 3. Simulation results for an airship as well as for a underwater vehicle model are contained in Section 4. Section 5 offers conclusions.

2. Dynamical model of vehicle in terms of generalized velocity components

The six DOF dynamical model of the considered here class of vehicles (Fig. 1) is expressed in the body-fixed reference frame by [18]:

$$M\dot{\nu}+C(\nu)\nu+D(\nu)\nu+g(\eta)=\tau, \quad (1)$$

$$\dot{\eta}=J(\eta)\nu, \quad (2)$$

where (1) is the vehicle dynamics and (2) is the kinematics. In these equations $M \in R^{6\times6}$ means the inertia matrix including the rigid body inertia matrix and the added mass matrix. Moreover, two conditions $M = M^T > 0$ and $\dot{M} = 0$ are fulfilled. However, we must take into account that vehicles are different. Therefore, the condition $\dot{M} = 0$ must be carefully checked for each considered object whether it is acceptable. Besides, $C(\nu) \in R^{6\times6}$ is the matrix of Coriolis and centrifugal terms (that satisfies $C(\nu) = -C^T(\nu), \forall \nu \in R^6$), $D(\nu) \in R^{6\times6}$ is the matrix of hydrodynamic damping terms ($D(\nu) > 0, \forall \nu \in R^6, \nu \neq 0$), $g(\eta) \in R^6$ is the vector of gravitational and buoyancy forces and moments,

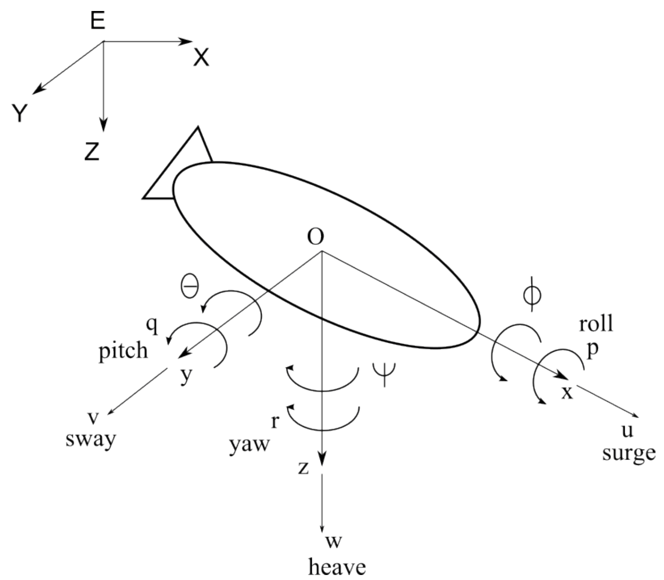

Fig. 1. Coordinate system for 6 DOF vehicle

$\eta \in R^6$ is the vector of positions and Euler angles, $\nu \in R^6$ is the vector of body-fixed linear and angular velocity components, and $\tau \in R^6$ is the control vector. The components of two vectors, namely $\nu = [u, v, w, p, q, r]^T$ and $\eta = [x, y, z, \phi, \theta, \psi]^T$ are related to the motion variable in surge, sway, heave, roll, pitch, and yaw, respectively. Additionally, $J(\eta)$ is a 6×6 block diagonal transformation matrix between the body-fixed frame to the inertial reference frame (usually the earth). The matrix $J(\eta)$ depends on the Euler angles.

Remark 1. Recall, that the inertia matrix M is constant, symmetric, and in general, non-diagonal, i.e. it contains off-diagonal elements. In order to obtain equations with a diagonal inertia matrix which allows us to design a decoupled controller in the sense that each rate can be regulated separately the matrix M should be decomposed. In general components of the inertia matrix depend on geometry, fluid flow rates and other uncertainties. Moreover, the added mass coefficients are often estimated using experimental studies and empirical relations which are not quite accurate. As a result, it should be stated that if the matrix M appears to be non-symmetric then it cannot be decomposed into a diagonal form and the proposed approach is not valid. Thus, the decomposition of the inertia matrix M (1) is possible if it is assumed that the matrix is symmetric, positive definite and their elements are known. As it arises from the literature [18] for a class of marine vehicle models such approximation is reasonable. Similarly conclusion can be made for indoor airships moving with low velocity.

Remark 2. Note that various moving systems can be described using Eqs. (1) and (2). Equations of this type are used for underwater vehicles [46, 2, 25, 47, 48] and for surface vessels [49, 7, 50, 8, 51, 11, 12]. However, hovercrafts [5, 52, 32, 53] as well as indoor airships [54–57] can be also described by these equations.

Introducing now a transformation of rates in the form:

$$\nu = \Upsilon\xi, \quad (3)$$

where Υ is an upper diagonal, invertible matrix with constant elements it is possible to decompose the matrix M into three matrices, i.e. $M = \Upsilon^{-T}N\Upsilon^{-1}$. The obtained matrix N is diagonal and it contains constant elements on the diagonal.

Calculating the time derivative of ν we have $\dot{\nu} = \Upsilon\dot{\xi}$. Taking the above into account and inserting (3) into (1), and next pre-multiplying both sides by Υ^T (as in [58]) we can write:

$$M\Upsilon\dot{\xi}+C(\nu)\Upsilon\xi+D(\nu)\Upsilon\xi+g(\eta)=\tau, \quad (4)$$

$$\Upsilon^T M\Upsilon\dot{\xi}+\Upsilon^T C(\nu)\Upsilon\xi+\Upsilon^T D(\nu)\Upsilon\xi+\Upsilon^T g(\eta)=\Upsilon^T\tau. \quad (5)$$

Grouping now the terms of the equation, the transformed equations of motion can be written in the following form:

$$N\dot{\xi}+C_\xi(\xi)\xi+D_\xi(\xi)\xi+g_\xi(\eta)=\pi, \quad (6)$$

$$\dot{\eta}=J(\eta)\Upsilon\xi, \quad (7)$$

where the appropriate matrices and vectors are given as follows:

$$N = \Upsilon^T M \Upsilon, \tag{8}$$

$$C_\xi(\xi) = \Upsilon^T C(\nu)\Upsilon, \tag{9}$$

$$D_\xi(\xi) = \Upsilon^T D(\nu)\Upsilon, \tag{10}$$

$$g_\xi(\eta) = \Upsilon^T g(\eta), \tag{11}$$

$$\pi = \Upsilon^T \tau. \tag{12}$$

Equations (6) and (3) together with (7) describe the motion of a vehicle, where N is a diagonal matrix. As it was mentioned in [59] there are various possible decomposition methods. However, in this work the Loduha-Ravani method which is related to the generalized velocity components (GVC) [60] is used (the obtained matrix Υ is only an upper triangular matrix containing ones on the diagonal).

3. Design of decoupled non-adaptive velocity tracking controller

In this section, the general controller decoupled in the sense of the vector of the transformed variables ξ is presented.

3.1. Control algorithm. The controller can be used for fully actuated underwater vehicles, hovercrafts or indoor airships. Moreover, it is assumed that the vehicle moves, i.e. the airship is in flight phase or the marine vehicle flows. Other motion phases are not taken into consideration.

Theorem 1. Consider the vehicle dynamic model (6), the kinematic relationship (7), and the velocity transformation (3) together with the following controller:

$$\begin{aligned} \pi = {} & N\dot{\xi}_r + C_\xi(\xi)\xi_r + D_\xi(\xi)\xi_r + \\ & + g_\xi(\eta) + k_D s_\xi + \Upsilon^T k_I z, \end{aligned} \tag{13}$$

where

$$z = \int_0^t \tilde{\nu}(\sigma)\, d\sigma, \tag{14}$$

$$\xi_r = \Upsilon^{-1}(\nu_d + \Lambda z), \tag{15}$$

$$s_\xi = \xi_r - \xi = \Upsilon^{-1}(\tilde{\nu} + \Lambda z), \tag{16}$$

$$\dot{s}_\xi = \dot{\xi}_r - \dot{\xi} = \Upsilon^{-1}(\dot{\tilde{\nu}} + \Lambda\tilde{\nu}), \tag{17}$$

and $\tilde{\nu} = \nu_d - \nu$ is the velocity error vector (the quantity with index d is related to the desired velocity whereas without the index to the actual velocity), $k_D = k_D^T > 0$, $k_I = k_I^T > 0$, $\Lambda = \Lambda^T > 0$, and N is a diagonal strictly positive matrix. The equilibrium point $[s_\xi^T, z^T]^T = 0$ is globally exponentially stable.

Remark 3. For simplicity we will assume that k_D, k_I, and Λ are constant and diagonal. Note also that the quantity s_ξ is analogous to the virtual velocity error vector s, whereas ξ_r is similar to the reference velocity vector defined by Slotine and Li [61]. However, because of the presence the matrix Υ we take here in to consideration also dynamics of the system. Moreover, for each considered vehicle we should take into account values of controlling forces and force moments. Thus, it is necessary to check these values for the vehicle.

Proof. The closed-loop system (6, 7) together with the controller (13) can be written as follows:

$$\begin{aligned} & N\dot{\xi} + C_\xi(\xi)\xi + D_\xi(\xi)\xi + g_\xi(\eta) = N\dot{\xi}_r + C_\xi(\xi)\xi_r \\ & + D_\xi(\xi)\xi_r + g_\xi(\eta) + k_D s_\xi + \Upsilon^T k_I z \end{aligned} \tag{18}$$

which leads to:

$$N\dot{s}_\xi + [C_\xi(\xi) + D_\xi(\xi) + k_D]s_\xi + \Upsilon^T k_I z = 0. \tag{19}$$

As a Lyapunov function candidate the following expression is proposed:

$$\mathscr{L}(s_\xi, z) = \frac{1}{2}s_\xi^T N s_\xi + \frac{1}{2}z^T k_I z. \tag{20}$$

Calculating the time derivative of the function $\mathscr{L}$ (20) leads to:

$$\dot{\mathscr{L}}(s_\xi, z) = s_\xi^T N\dot{s}_\xi + \frac{1}{2}s_\xi^T \dot{N} s_\xi + \tilde{\nu}^T k_I z. \tag{21}$$

Because the matrices M, and Υ have only constant elements, thus $\dot{N} = \frac{d}{dt}(\Upsilon^T M \Upsilon) = 0$. Using also the relationship (19) one gets:

$$\begin{aligned} \dot{\mathscr{L}}(s_\xi, z) = {} & s_\xi^T[-C_\xi(\xi)s_\xi - D_\xi(\xi)s_\xi - \\ & - k_D s_\xi - \Upsilon^T k_I z] + \tilde{\nu}^T k_I z. \end{aligned} \tag{22}$$

Recall, however (9), that $s_\xi^T C_\xi(\xi) s_\xi = (\Upsilon s_\xi)^T C(\nu)(\Upsilon s_\xi) = s^T C(\nu) s = 0$ (assuming $s = \Upsilon s_\xi$) because $s^T C(\nu) s = 0$ for all $s \in R^n$ (the matrix $C(\nu)$ is a skew-symmetric one) [18]. Therefore, taking into account (16) we have:

$$\begin{aligned} \dot{\mathscr{L}}(s_\xi, z) & = -s_\xi^T[D_\xi(\xi) + k_D]s_\xi - s_\xi^T \Upsilon^T k_I z + \tilde{\nu}^T k_I z \\ & = -s_\xi^T[D_\xi(\xi) + k_D]s_\xi - z^T \Lambda^T k_I z. \end{aligned} \tag{23}$$

The above result we can write in the following form (using (10)):

$$\dot{\mathscr{L}}(s_\xi, z) = -\begin{bmatrix} s_\xi \\ z \end{bmatrix}^T \underbrace{\begin{bmatrix} A_{11} & 0 \\ 0 & A_2 \end{bmatrix}}_{A} \begin{bmatrix} s_\xi \\ z \end{bmatrix}, \tag{24}$$

where $A_{11} = \Upsilon^T D(\nu)\Upsilon + k_D$ and $A_{22} = \Lambda^T k_I$. Note that the symmetric matrix A is positive definite. Thus, assuming $\lambda_m\{A\} > 0$ (λ_m is the minimal eigenvalue of the matrix A) one can find an upper bound of the time derivative. Denoting now $x = [s_\xi^T, z^T]^T$ one can write:

$$\dot{\mathscr{L}}(t,x) \leq -\lambda_m\{A\}||x||^2, \tag{25}$$

for all $t \geq 0$ and $x \in R^{2\mathscr{N}}$.
Therefore, based on the Lyapunov direct method [61], the conclusion that the state space origin of the system (6), (3) together with the controller (13):

$$\lim_{t\to\infty} \begin{bmatrix} s_\xi(t) \\ z(t) \end{bmatrix} = 0, \tag{26}$$

is globally exponentially convergent can be made.

3.2. Robustness issue. In case of vehicle parameters uncertainty we must consider robustness of the proposed control algorithm. The sensitivity analysis will be done using the relationships between the variables in the given below way.

Taking into account inversion of the relationship (12) and (14–17) (note that $\tau = \Upsilon^{-T}\pi$) the input forces vector τ can be rewritten as follows:

$$\begin{aligned}\tau = M(\dot{v}_d + \Lambda\tilde{v}) + C(v)(v_d + \Lambda z) + D(v)(v_d + \Lambda z)\\ + g(\eta) + \Upsilon^{-T} k_D \Upsilon^{-1}(\tilde{v} + \Lambda z) + k_I z.\end{aligned} \tag{27}$$

Denoting now $v_r = v_d + \Lambda z$, $\dot{v}_r = \dot{v}_d + \Lambda\tilde{v}$, and $s = \tilde{v} + \Lambda z$ we are able to rewrite the above equation in the form:

$$\begin{aligned}\tau = M\dot{v}_r + C(v)v_r + D(v)v_r + g(\eta)\\ + \Upsilon^{-T} k_D \Upsilon^{-1} s + k_I z.\end{aligned} \tag{28}$$

Note that comparing (13) we have the relationships:

$$s = \Upsilon s_\xi, \quad s = v_r - v, \quad \dot{s} = \dot{v}_r - \dot{v}. \tag{29}$$

Thus, we reformulate the Lyapunov function candidate as follows:

$$\mathscr{L} = \frac{1}{2} s_\xi^T N s_\xi + \frac{1}{2} z^T k_I z = \frac{1}{2} s^T M s + \frac{1}{2} z^T k_I z. \tag{30}$$

Its time derivative has the form:

$$\dot{\mathscr{L}} = s^T M \dot{s} + \tilde{v}^T k_I z = s^T(M\dot{v}_r - M\dot{v}) + \tilde{v}^T k_I z. \tag{31}$$

Assuming for simplification $C = C(v)$, $D = D(v)$, $g = g(\eta)$ and using (29) we receive the given below equation:

$$\begin{aligned} M\dot{v} &= \tau - Cv - Dv - g \\ &= \tau - C(v_r - s) - D(v_r - s) - g. \end{aligned} \tag{32}$$

Hence, recalling that $s^T C s = 0$ [18] we obtain:

$$\begin{aligned}\dot{\mathscr{L}} &= s^T M \dot{s} + \tilde{v}^T k_I z = s^T(M\dot{v}_r - M\dot{v}) + \tilde{v}^T k_I z \\ &= s^T(M\dot{v}_r + Cv_r + Dv_r + g - Ds - \tau) + \tilde{v}^T k_I z.\end{aligned} \tag{33}$$

Let now define the control input in the following form:

$$\tau = \hat{M}\dot{v}_r + \hat{C}v_r + \hat{D}v_r + \hat{g} + \hat{\Upsilon}^{-T} k_D \hat{\Upsilon}^{-1} s + k_I z. \tag{34}$$

where the parameters in $\hat{M}$, $\hat{C}$, $\hat{D}$, $\hat{g}$, $\hat{\Upsilon}^{-T}$, and $\hat{\Upsilon}^{-T}$ are known. Inserting (34) into (33) we receive:

$$\begin{aligned}\dot{\mathscr{L}} = s^T[(M - \hat{M})\dot{v}_r + (C - \hat{C})v_r + (D - \hat{D})v_r\\ + g - \hat{g} - Ds - \hat{\Upsilon}^{-T} k_D \hat{\Upsilon}^{-1} s - k_I z] + \tilde{v}^T k_I z.\end{aligned} \tag{35}$$

Denoting now $\tilde{M} = \hat{M} - M$, $\tilde{C} = \hat{C} - C$, $\tilde{D} = \hat{D} - D$, $\tilde{g} = \hat{g} - g$, and using the expression $s = \Upsilon s_\xi$ (the signals obtained from the controller) we get:

$$\begin{aligned}\dot{\mathscr{L}} &= -s^T(\tilde{M}\dot{v}_r + \tilde{C}v_r + \tilde{D}v_r + \tilde{g}) - (\tilde{v}^T + z^T\Lambda^T)k_I z \\ &\quad - s^T(D + \hat{\Upsilon}^{-T} k_D \hat{\Upsilon}^{-1})s + \tilde{v}^T k_I z = -s^T(\tilde{M}\dot{v}_r \\ &\quad + \tilde{C}v_r + \tilde{D}v_r + \tilde{g}) - s^T(D + \hat{\Upsilon}^{-T} k_D \hat{\Upsilon}^{-1})s \\ &\quad - z^T\Lambda^T k_I z = -s_\xi^T \hat{\Upsilon}^T(\tilde{M}\dot{v}_r + \tilde{C}v_r + \tilde{D}v_r + \tilde{g}) \\ &\quad - s_\xi^T \hat{\Upsilon}^T(D + \hat{\Upsilon}^{-T} k_D \hat{\Upsilon}^{-1})\hat{\Upsilon} s_\xi - z^T\Lambda^T k_I z.\end{aligned} \tag{36}$$

Based on [61] we can find the strictly positive constants β_i, where $i = 1, \ldots, 6$ in order to ensure convergence of the tracking error to zero. Therefore, choosing $\beta_i \geq |[\hat{\Upsilon}^T(\hat{M}\dot{v}_r + \tilde{C}v_r + \hat{D}v_r + \tilde{g})]_i|$ we receive (assuming k_D and $\Lambda^T k_I$ as symmetric or diagonal matrices):

$$\begin{aligned}\dot{\mathscr{L}} \leq -\sum_{i=1}^{6} \beta_i |s_{\xi\,i}| - s_\xi^T \hat{\Upsilon}^T(D + \hat{\Upsilon}^{-T} k_D \hat{\Upsilon}^{-1})\hat{\Upsilon} s_\xi \\ - z^T\Lambda^T k_I z.\end{aligned} \tag{37}$$

This condition leads us to conclusion that the tracking error convergence is guaranteed for $t \to \infty$ if the vehicle dynamics is not exactly known.

3.3. Some properties and advantages of decoupled controller. The proposed controller, which is non-interacting in the sense of the quasi-acceleration vector, gives some useful advantages. Consider the practical interest of the controller.

1. From (27) we observe that the gain matrix $K_D = \Upsilon^{-T} k_D \Upsilon^{-1}$ includes also dynamics of the system. Consequently, the input signal τ is strictly related not only to kinematics but also to the vehicle dynamics. This means that the matrix k_D is chosen according to dynamics of the controlled plant (e.g for a heavy vehicle the control coefficients can be different than for a light vehicle). Even if the system parameters are not exactly known, thanks to the matrix Υ, the velocity error decreases quickly.
2. The diagonal inertia matrix N gives information about the inertia related to each quasi-acceleration (without dynamical couplings). Moreover, each quasi-velocity ξ_i is inde-

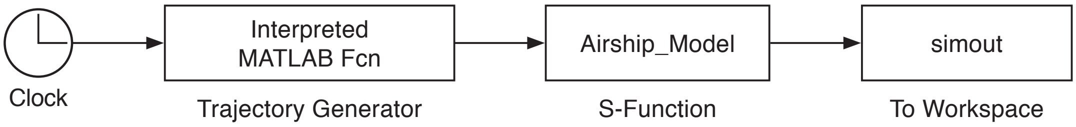

Fig. 2. Diagram of the control strategy in in MATLAB/Simulink environment for the tested airship

pendent from other quasi-velocities and allows one to determine the kinetic energy reduced by the variable ξ_i, i.e. $K(\xi) = \frac{1}{2}\nu^T M \nu = \frac{1}{2}\xi^T N \xi = \frac{1}{2}\sum_{i=1}^{6} N_i \xi_i^2$. These independent quasi-velocities are used in the proposed decoupled controller.

3. Some particular cases of the presented controller can be deduced. We can point at two cases:
   (a) For a symmetric vehicle in the xy-plane we get $y_g = 0$; as a results the controller is simplified and reduced. Consequently, the impact of dynamic couplings effect is reduced, too.
   (b) The matrix M is a diagonal one. It such case the simplified form is as follows:

$$\tau = M\dot{\nu}_r + C(\nu)\nu_r + D(\nu)\nu_r + g(\eta) + k_D s + k_I z \tag{38}$$

because we obtain $\Upsilon = I$ (the identity matrix).

4. Simulation results

4.1. Indoor airship model. In this section we present some results regarding the use of the proposed controller for the model of airship AS500 (assuming indoor test with low velocity). The simulations were done in MATLAB/Simulink environment for 6 DOF model with six signal inputs. The blimp parameters coming from the report [62] were also applied in [63]. The maximal forces and torques applied by the control system were assumed as follows: $F_{max\,x,y,z} = 107, 13, 40$ N, $T_{max\,x,y,z} = 27, 267, 27$ Nm. The values were taken from [64] for the airship AS800 (both airships have similar construction). The diagram of the control strategy is presented in Fig. 2.

Case 1 – set of nominal parameters. In this example the nominal parameters set of the airship is taken into account. The task relies on tracking the velocity trajectory described by:

$$\nu_d = [\sin(\pi/20 \cdot t) + 2,\ 0,\ \sin(\pi/25 \cdot t),\ 0,\ 0,\ 0.1 \cdot \cos(pi/15 \cdot t)]^T. \tag{39}$$

The set of selected gains for the nonlinear controller is as follows:

$$k_D = \mathrm{diag}\{95, 95, 95, 60, 60, 60\}, \tag{40}$$

$$k_I = \mathrm{diag}\{85, 85, 85, 60, 60, 60\}, \tag{41}$$

$$\Lambda = \mathrm{diag}\{0.35, 0.35, 0.35, 1.0, 1.0, 1.0\}, \tag{42}$$

The desired linear and angular velocities profiles are given in Fig. 3 a) and b), respectively. Note that three profiles change during the airship motion according to sinusoidal functions. Next, in Fig. 3 a) each linear velocity error time history is presented. The error decreases, as it was expected, quickly and

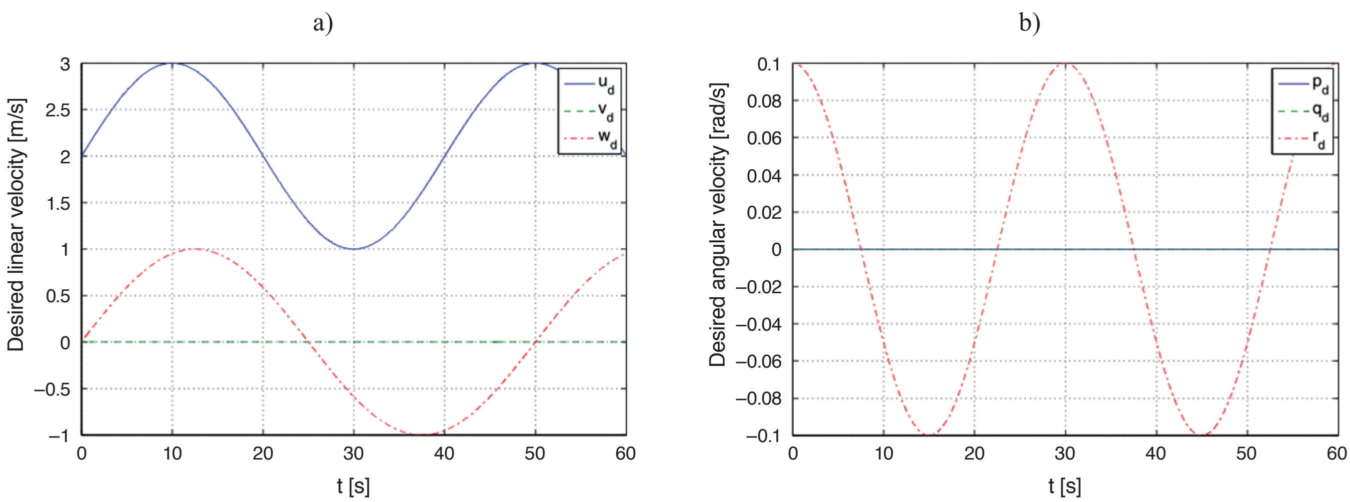

Fig. 3. Case 1 and Case 2: a) desired linear velocities u_d, v_d, w_d, b) desired angular velocities p_d, q_d, r_d

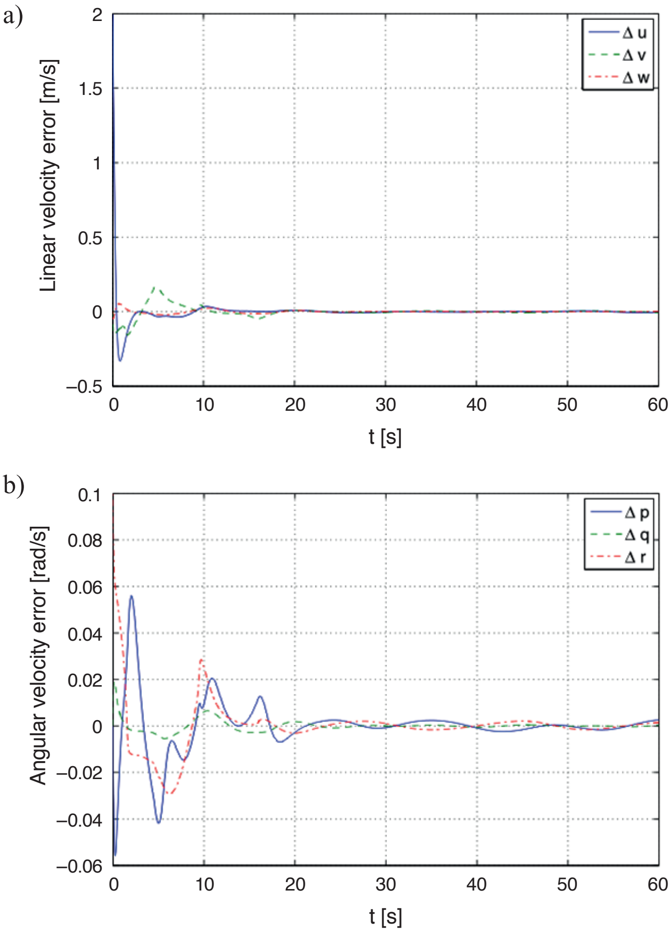

Fig. 4. Case 1 ($\Delta v \equiv \tilde{v}$): a) linear velocity errors Δu, Δv, Δw, b) angular velocity errors Δp, Δq, Δr

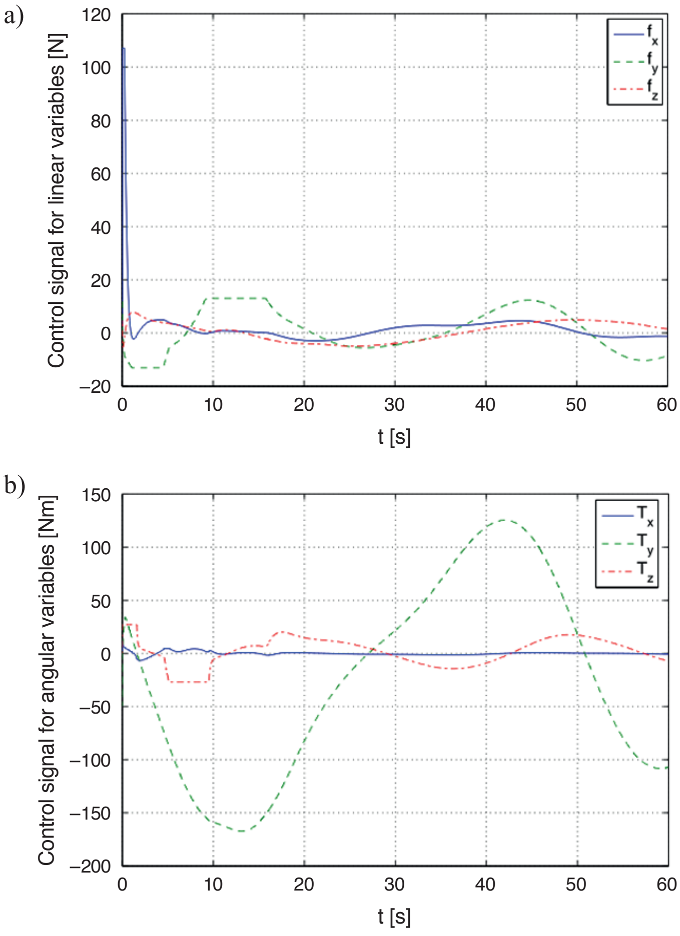

Fig. 5. Case 1 – control signals: a) applied forces f_x, f_y, f_z, b) applied torques T_x, T_y, T_z

after about 30 second the error is close to zero. In Fig. 4 b) the angular velocity errors for angular variables are shown. The error reduction is not so fast as the linear velocity error but after about 20 second all signals are significantly reduced. It arises from the fact that part of dynamical couplings is taken into account in the control algorithm. However, because the angular velocity trajectory changes sinusoidal the error is only close to zero. The control signals related to linear velocity variables are reported in Fig. 5 a). Their values after short time are below 20 N. From Fig. 5 b) we see that the applied torque T_y

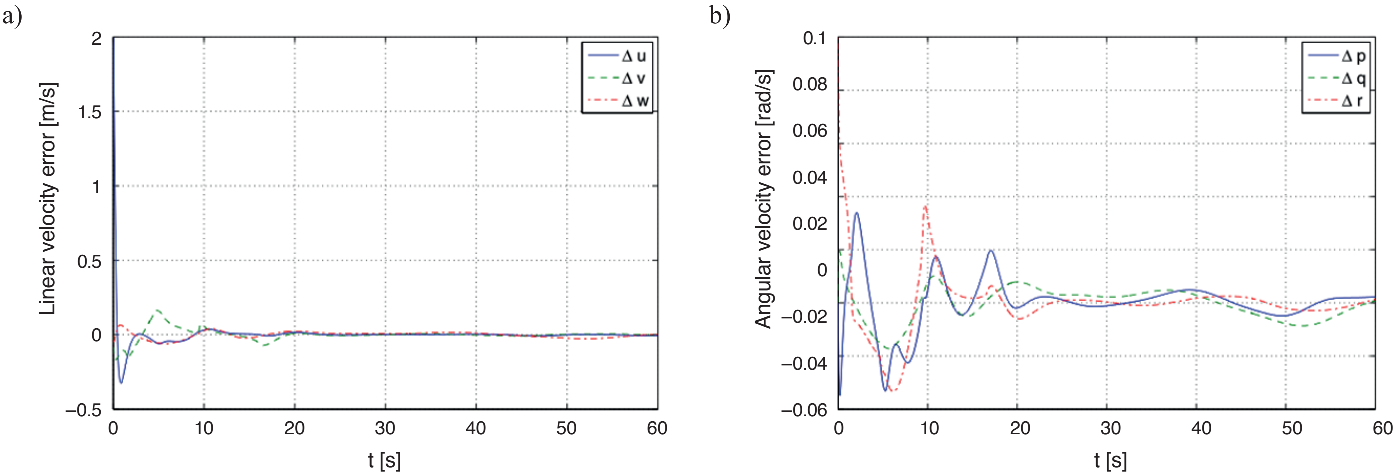

Fig. 6. Case 2 – 50% weight reduction ($\Delta v \equiv \tilde{v}$): a) linear velocity errors Δu, Δv, Δw, b) angular velocity errors Δp, Δq, Δr

a)

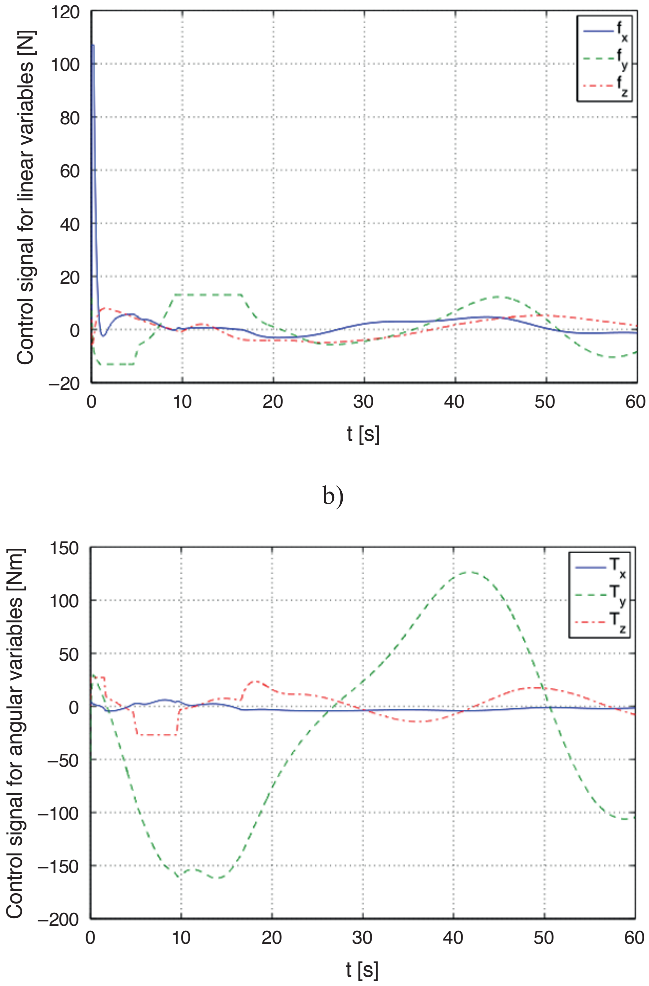

Fig. 7. Case 2 – 50% weight reduction, control signals: a) applied forces f_x, f_y, f_z, b) applied torques T_x, T_y, T_z

has during the motion maximal value over 100 Nm. It can be concluded that the dynamical couplings affect the movement in this direction.

Case 2 (robustness test) – 50% weight reduction. In order to investigate sensitivity to the parameter changes of the controller the robustness test was done. It was assumed that the blimp weight has been reduced to 50%. Such situation may result from loss of gas in the blimp or if not all parameters are known exactly. The desired velocity was the same as for the nominal parameters set.

The linear velocity errors are shown in Fig. 6 a) whereas the angular velocity errors in Fig. 6 b). Similarly, as previously the decreasing of the initial errors is great. In spite of the fact that their values after about 30 s are slightly bigger than for the case of nominal parameters, the controller works still correctly with acceptable performance. From Fig. 7 a) and Fig. 7 b), it arises that the forces and torques have comparable values as in Case 1. These observations lead us to conclusion that the proposed control algorithm is robust to parameter changes.

4.2. Underwater vehicle model. The simulations were done for 6 DOF model of underwater vehicle which parameters can be found in [58].

Case 3 – set of nominal parameters. In this example the nominal parameters are used and the velocity tracking trajectory is described by (39). The aim is to show that the proposed control scheme is appropriate also for marine vehicles.

The control gains selected for velocity tracking task are as follows:

$$k_D = \text{diag}\{10, 10, 10, 10, 10, 10\}, \tag{43}$$

$$k_I = \text{diag}\{10, 10, 10, 10, 10, 10\}, \tag{44}$$

$$\Lambda = \text{diag}\{1.5, 1.5, 1.5, 1.5, 1.5, 1.5\}, \tag{45}$$

They are different than for the airship because the dynamics of these two vehicles is quite different. Moreover, the control gains are directly related to the system dynamics.

In Fig. 8 a) three linear velocity errors are shown. We observe that the Δu tends to zero after about 7 s, while the others are close to zero at the beginning of the movement. From Fig. 8

a)

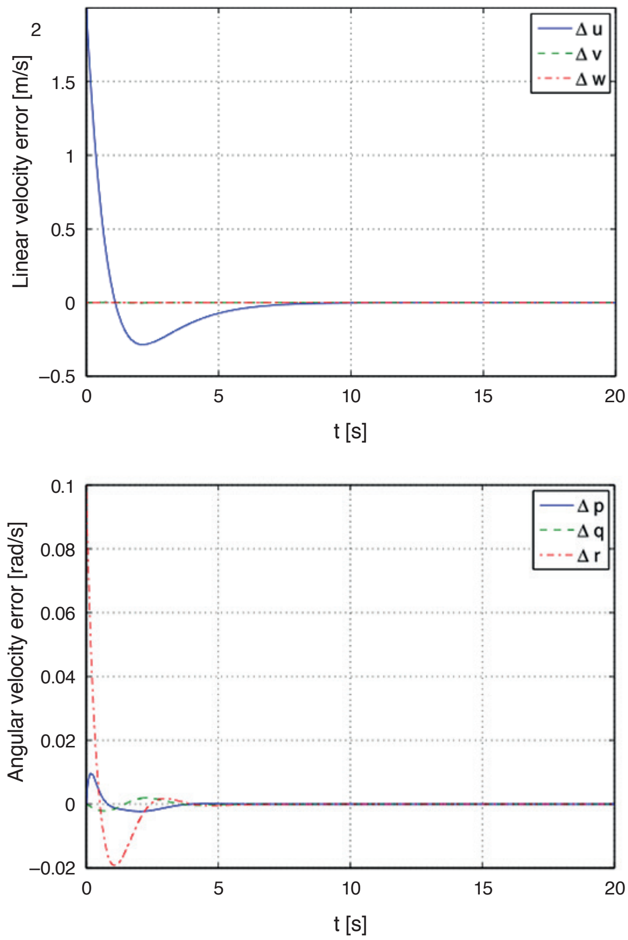

Fig. 8. Case 3 ($\Delta v \equiv \tilde{v}$): a) linear velocity errors Δu, Δv, Δw, b) angular velocity errors Δp, Δq, Δr

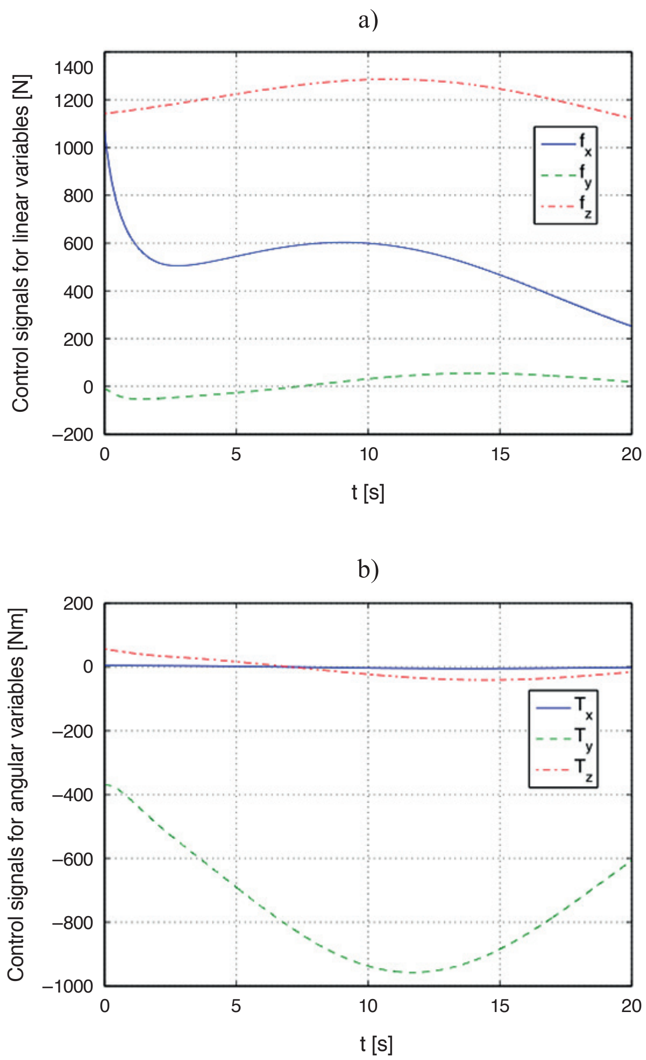

Fig. 9. Case 3 – control signals: a) applied forces f_x, f_y, f_z, b) applied torques T_x, T_y, T_z

b) we see that all angular velocity errors are reduced to zero after about 5 s. We can note that the dynamical coupling causes that at the start all variables are actuated (in spite of that only is r tracked). The velocity tracking without overshoot can be explained by the strong mechanical couplings and great mass of the vehicle ($m = 250$ kg [58], whereas $m = 18.375$ kg [62] for the airship). Observing the control signals time history related to linear velocity variables given in Fig. 9 a) we see the greatest force changes for the f_x. It arises from the fact that in the initial point the velocity is $+2$ [m/s] and next it is reduced. From Fig. 9 b) it is noticeable that the applied torque T_y has the greatest values. This fact can be explained by strong dynamical couplings which act in this direction.

5. Conclusions

A velocity tracking controller based on Lyapunov techniques has been derived in this work. The controller can be used for various fully actuated vehicles, namely marine (underwater) vehicles, hovercrafts or indoor airships moving with low velocity. Its robustness was discussed and formally proven. It was also mentioned that simpler controllers can be deduced from the controller discussed. Simulation results for both 6 DOF airship and underwater vehicle model show effectiveness of the proposed methodology.

Acknowledgments. The work was funded by the National Science Centre of Poland by decision DEC-2011/03/B/ST7/02524 and it was supported by the University Grant No. 09/93/DSPB/0611.

References

[1] G. Antonelli, F. Caccavale, S. Chiaverini, and G. Fusco, "A novel adaptive control law for underwater vehicles", *IEEE Transactions on Control Systems Technology* 11 (2), 221–232 (2003).

[2] G. Conte and A. Serrani, "Robust nonlinear motion control for AUVs", *IEEE Robotics and Automation Magazine* 6 (2), 33–38 and 62 (1999).

[3] N. Fischer, D. Hughes, P. Walters, E.M Schwartz., and W.E. Dixon, "Nonlinear RISE-based control of an autonomous underwater vehicle", *IEEE Transactions on Robotics* 30 (4), 845–852 (2014).

[4] O.-E. Fjellstad and T.I. Fossen, "Position and attitude tracking of AUVs: A quaternion feedback approach", *IEEE Journal of Oceanic Engineering* 19 (4), 512–518 (1994).

[5] A.P. Aguiar, L. Cremean, and J.P. Hespanha, "Position tracking for a nonlinear underactuated hovercraft: Controller design and experimental results", *Proc. 42nd IEEE Conference on Decision and Control*, 3858–3863 (2003).

[6] H. Ashrafiuon, K.R. Muske, L.C. McNinch, and R.A. Soltan, "Sliding-mode tracking control of surface vessels", *IEEE Transactions on Industrial Electronics* 55 (11), 4004–4012 (2008).

[7] D. Chwa, "Global tracking control of underactuated ships with input and velocity constraints using dynamic surface control method", *IEEE Transactions on Control Systems Technology* 19 (6), 1357–1370 (2011).

[8] K.D. Do, Z.P. Jiang, and J. Pan, "Global partial-state feedback and output-feedback tracking controllers for underactuated ships", *Systems and Control Letters* 54, 1015–1036 (2005).

[9] J.-M. Godhavn, "Nonlinear tracking of underactuated surface vessels", *Proc. 35th IEEE Conference on Decision and Control*, 975–980 (1996).

[10] J.-M. Godhavn, T.I. Fossen, and S.P. Berge, "Non-linear and adaptive backstepping designs for tracking control of ships", *International Journal of Adaptive Control and Signal Processing* 12, 649–670 (1998).

[11] Z.-P. Jiang, "Global tracking control of underactuated ships by Lyapunov's direct method", *Automatica* 38, 301–309 (2002).

[12] E. Lefeber, K.Y. Pettersen, and H. Nijmeijer, "Tracking control of an underactuated ship", *IEEE Transactions on Control Systems Technology* 11 (1), 52–61 (2003).

[13] K.Y. Pettersen and H. Nijmeijer, "Underactuated ship tracking control: Theory and experiments", *International Journal of Control* 74 (14), 1435–1446 (2001).

[14] H. Sira-Ramirez, "Dynamic second-order sliding mode control of the hovercraft vessel", *IEEE Transactions on Control Systems Technology* 10 (6), 860–865 (2002).

[15] M. Wondergem, E. Lefeber, K.Y. Pettersen, and H. Nijmeijer, “Output feedback tracking of ships”, *IEEE Transactions on Control Systems Technology* 19 (2), 442–448 (2011).
[16] H. Ashrafiuon, K.R. Muske, and L.C. McNinch, “Review of nonlinear tracking and setpoint control approaches for autonomous underactuated marine vehicles”, *Proc. 2010 American Control Conference*, 5203–5211 (2010).
[17] K.D. Do and J. Pan, *Control of Ships and Underwater Vehicles*, Springer-Verlag, London, 2009.
[18] T.I. Fossen, *Guidance and Control of Ocean Vehicles*, John Wiley and Sons, Chichester, 1994.
[19] S. Soylu, A.A Proctor, R.P. Podhorodeski, C. Bradley, and B.J. Buckham, “Precise trajectory control for an inspection class ROV”, *Ocean Engineering* 111, 508–523 (2016).
[20] N. Wang, C. Qian, J.-C. Sun, and Y.-C. Liu, “Adaptive robust finite-time trajectory tracking control of fully actuated marine surface vehicles”, *IEEE Transactions on Control Systems Technology* 24 (4), 1454–1462 (2016).
[21] T. Fukao, K. Fujitani, and T. Kanade, “Image-based tracking control of a blimp”, *Proc. 42nd IEEE Conference on Decision and Control*, 5414–5419 (2003).
[22] T. Fukao, T. Kanzawa, and K. Osuka, “Tracking control of an aerial blimp robot based on image information”, *Proc. 16th IEEE International Conference on Control Applications*, 874–879 (2007).
[23] D. Han, X.-l. Wang, L. Chen, and D.-p. Duan, “Command-filtered backstepping control for a multi-vectored thrust stratospheric airship”, *Transactions of the Institute of Measurement and Control* 38 (1), 93–104 (2016).
[24] E.C. de Paiva, J.R. Azinheira, J.G. Ramos Jr., A. Moutinho, and S.S. Bueno, “Project AURORA: Infrastructure and flight control experiments for a robotic airship”, *Journal of Field Robotics* 23 (3/4), 201–222 (2006).
[25] L.G. Garcia-Valdovinos, T. Salgado-Jimenez, M. Bandala-Sanchez, L. Nava-Balanzar, R. Hernandez-Alvarado, and J.A. Cruz-Ledesma, “Modelling, design and robust control of a remotely operated underwater vehicle”, *International Journal of Advanced Robotic Systems* 11 (1), 1–16 (2014).
[26] J. Nie, J. Yuh, E. Kardash, and T.I. Fossen, “On-board sensor-based adaptive control of small UUVs in very shallow water”, *International Journal of Adaptive Control and Signal Processing* 14, 441–452 (2000).
[27] E. Sebastián and M.A. Sotelo, “Adaptive fuzzy sliding mode controller for the kinematic variables of an underwater vehicle”, *Journal of Intelligent Robotic Systems* 49, 189–215 (2007).
[28] D.R. Yoerger and J.-J.E. Slotine, “Robust trajectory control of underwater vehicles”, *IEEE Journal of Oceanic Engineering* 10 (4), 462–470 (1985).
[29] J. Yuh, J. Nie, and C.S.G. Lee, “Experimental study on adaptive control of underwater robots”, *Proc. 1999 IEEE International Conference on Robotics & Automation*, 393–398 (1999).
[30] R. Skjetne, T.I. Fossen, and P.V. Kokotovic, “Adaptive maneuvering, with experiments, for a model ship in a marine control laboratory”, *Automatica* 41, 289–298 (2005).
[31] K.P. Tee and S.S. Ge, “Control of fully actuated ocean surface vessels using a class of feedforward approximators”, *IEEE Transactions on Control Systems Technology* 14 (4), 750–756 (2006).
[32] R. Hayashi, K. Osuka, and T. Ono, “Trajectory control of an air cushion Vehicle”, *Proc. IEEE/RSJ/GI International Conference on Intelligent Robots and Systems ’94. ‘Advanced Robotic Systems and the Real World’*, 1906–1913 (1994).
[33] F. Ruffier, T. Mukai, H. Nakashima, J. Serres, and N. Franceschini, “Combining sound and optic flow cues to reach a sound source despite lateral obstacles”, *2008 IEEE/SICE International Symposium on System Integration*, 89–94 (2008).
[34] A. Moutinho, L. Mirisola, J. Azinheira, and J. Dias, “Project DIVA: Guidance and vision surveillance techniques for an autonomous airship”, in *Robotics Research Trends*, pp. 77–120, ed. X. P. Guo, Nova Science Publishers, Inc., New York, 2007.
[35] L. Solaque and S. Lacroix, “Airship control”, in *Multiple Heterogeneous Unmanned Aerial Vehicles*, pp. 147–188, eds. A. Ollero and I. Maza, STAR 37, 2007.
[36] T. Yamasaki and N. Goto, “Identification of blimp dynamics via flight tests”, *Transactions of the Japan Society for Aeronautical and Space Sciences* 46 (153), 195–205 (2003).
[37] T.I. Fossen and O.-E. Fjellstad, “Cascaded adaptive control of ocean vehicles with significant actuator dynamics”, *Proc. 12th IFAC World Congress on Automatic Control*, 517–522 (1993).
[38] M. Breivik, *Topics in Guided Motion Control of Marine Vehicles*, PhD Thesis, Norwegian University of Science and Technology, Trondheim, 2010.
[39] M. Breivik, V.E. Hovstein, and T.I. Fossen, “Straight-line target tracking for unmanned surface vehicles”, *Modeling, Identification, and Control* 29 (4), 131–149 (2008).
[40] B. Ferreira, A. Matos, N. Cruz, and M. Pinto, “Modeling and control of the mares autonomous underwater vehicle”, *Marine Technology Society Journal* 44 (2), 19–36 (2010).
[41] F. Mahini, L. DiWilliams, K. Burke, and H. Ashrafiuon, “An experimental setup for autonomous operation of surface vessels in rough seas”, *Robotica* 31, 703–715 (2013).
[42] L.C. McNinch and H. Ashrafiuon, “Predictive and sliding mode cascade control for unmanned surface vessels”, *Proc. 2011 American Control Conference*, 184–189 (2011).
[43] H.R. Pota, B. Ahmed, and M. Garratt, “Velocity control of a UAV using backstepping control”, *Proc. 45th IEEE Conference on Decision and Control*, 5894–5899 (2006).
[44] A.E. Neff, D. Lee, V.K. Chitrakaran, D.M. Dawson, and T.C. Burg, “Velocity control for a quad-rotor UAV fly-by-camera interface”, *Proc. IEEE SoutheastCon 2007*, 273–278 (2007).
[45] K. Tchoń, K. Zadarnowska, Ł. Juszkiewicz, and K. Arent, “Modeling and control of a skid-steering mobile platform with coupled side wheels”, *Bull. Pol. Ac.: Tech.* 63 (3), 807–818 (2015).
[46] F. Alonge, F. D’Ippolito, and F.M. Raimondi, “Trajectory tracking of underactuated underwater vehicles”, *Proc. 44th IEEE Conference on Decision and Control*, 4421–4426 (2001).
[47] L. Lapierre and D. Soetanto, “Nonlinear path-following control of an AUV”, *Ocean Engineering* 34, 1734–1744 (2007).
[48] M.J. Paulsen, O. Egeland, and T.I. Fossen, “An output feedback controller with wave filter for marine vehicles”, *Proc. American Control Conference*, 2202–2208 (1994).
[49] A. Behal, D.M. Dawson, W.E. Dixon, and Y. Fang, “Tracking and regulation control of an underactuated surface vessel with nonintegrable dynamics”, *IEEE Transactions on Automatic Control* 47 (3), 495–500 (2002).
[0] K.D. Do, Z.P. Jiang, and J. Pan, “Universal controllers for stabilization and tracking of underactuated ships”, *Systems and Control Letters* 47, 299–317 (2002).
[51] Y. Fang, E. Zergeroglu, M.S. de Queiroz, and D.M. Dawson, “Global output feedback control of dynamically positioned surface vessels: An adaptive control approach”, *Mechatronics* 14, 341–356 (2004).
[52] I. Fantoni, R. Lozano, F. Mazenc, and K.Y. Pettersen, “Stabilization of a nonlinear underactuated hovercraft”, *International Journal of Robust and Nonlinear Control* 10, 645–654 (2000).

[53] R. Munoz-Mansilla, D. Chaos, J. Aranda, and J.M. Díaz, "Application of quantitative feedback theory techniques for the control of a non-holonomic underactuated hovercraft", *IET Control Theory and Applications* 6 (14), 2188–2197 (2012).

[54] S. Oh, S. Kang, K. Lee, S. Ahn, and E. Kim, "Flying display: Autonomous blimp with real-time visual tracking and image projection", *Proc. 2006 IEEE/RSJ International Conference on Intelligent Robots and Systems*, 131–136 (2006).

[55] Y. Ohata, S. Ushijima, and D.N. Nenchev, "Development of an indoor blimp robot with internet-based teleoperation capability", *Proc. 13th IASTED International Conference on Robotics and Applications*, 186–191 (2007).

[56] J.-C. Zufferey, A. Guanella, A. Beyeler, and D. Floreano, "Flying over the reality gap: From simulated to real indoor airships", *Autonomous Robots* 21, 243–254 (2006).

[57] S. Zwaan van der, A. Bernardino, and J. Santos-Victor, "Vision-based station keeping and docking for an aerial Blimp", *Proc. 2000 IEEE/RSJ International Conference on Intelligent Robots and Systems*, 614–619 (2000).

[58] P. Herman, "Decoupled PD set-point controller for underwater vehicles", *Ocean Engineering* 36, 529–534 (2009).

[59] P. Herman, "Transformed equations of motion for underwater vehicles", *Ocean Engineering* 36, 306–312 (2009).

[60] T.A. Loduha and B. Ravani, "On first-order decoupling of equations of motion for constrained dynamical systems", *Transactions of the ASME Journal of Applied Mechanics* 62, 216–222 (1995).

[61] J.-J. Slotine and W. Li, *Applied Nonlinear Control*, Prentice Hall, New Jersey, 1991.

[62] Y. Bestaoui, *Dynamique Dirigeable AS500 Complete Archive*, 2007, (unpublished).

[63] W. Adamski, P. Herman, Y. Bestaoui, and K. Kozlowski, "Control of airship in case of unpredictable environment conditions", *Proc. 2010 Conference on Control and Fault Tolerant* Systems, 843–848 (2010).

[64] J.R. Azinheira and A. Moutinho, "Hover control of an UAV with backstepping design including input saturations", *IEEE Transactions on Control Systems Technology* 16(3), 517–526 (2008).